Synthesis, Crystal Structure and Electronic Properties of a 2Fe–2S Complex with a Bulky Thiolato Ligand, $[NEt_4]_2[Fe_2S_2(SC_6H_2Me_3\text{-}2,4,6)_4]$ †

Norikazu Ueyama,[a] Satoru Ueno,[a] Takashi Sugawara,[a] Kazuyuki Tatsumi,[a] Akira Nakamura *,[a] and Noritake Yasuoka[b]

[a] *Department of Macromolecular Science, Faculty of Science, Osaka University, Toyonaka, Osaka 560, Japan*
[b] *Basic Research Institute, Himeji Institute of Technology, Himejishi 671-22, Japan*

The complex $[NEt_4]_2[Fe_2S_2(tmbt)_4]$ (tmbt = 2,4,6-trimethylbenzenethiolate) was synthesised and its molecular structure determined. The crystal system is monoclinic with $a = 15.241(6)$, $b = 16.174(5)$, $c = 16.768(6)$ Å, $\beta = 135.84(2)$ and $Z = 2$, in space group $P2_1/c$. The Fe–S* (S* = inorganic sulphide) bond lengths are 2.195(6) and 2.204(6) Å and the Fe–S(C) are 2.299(8) and 2.318(6) Å. Steric congestion at the thiolato ligands causes rotation of two of the four Fe–S(C) torsion angles from the stable staggered position to the restrictedly eclipsed position. The eclipsed Fe–S(C) has a wide Fe–S–C angle [112.35(76)°] with π-bond character and another staggered Fe–S(C) possesses a narrow Fe–S–C angle [104.95(64)°] with less π-bond character.

Biologically important plant-type ferredoxins have an $Fe_2S_2^{2+}$ core co-ordinated by four cysteine residues. Their redox potentials range from −0.23 to −0.42 V *vs.* normal hydrogen electrode (NHE).[1] Many model complexes with alkane- and arene-thiolate ligands, *etc.*, have been synthesised,[2–4] which include $[Fe_2S_2\{o\text{-}(SCH_2)_2C_6H_4\}_2]^{2-}$,[2] $[Fe_2S_2(SC_6H_4Me\text{-}p)_4]^{2-}$,[3] $[Fe_2S_2(SPh)_4]^{2-}$ [2] and $[Fe_2S_2(SePh)_4]^{2-}$.[4] These complexes have exhibited relatively negative redox potentials for the 3−/2− redox couple in organic solvents, for example, −1.49 V *vs.* saturated calomel electrode (SCE) in dimethylformamide (dmf).[2] The complex $[Fe_2S_2(PhCH_2OCO\text{-}Cys\text{-}X\text{-}Y\text{-}Cys\text{-}OMe)_2]^{2-}$ (X-Y = Ala-Ala, Ala-Pro or Pro-Leu), in which the peptide ligand chelates to one of the two iron ions of the $Fe_2S_2^{2+}$ core, was found to exhibit a positive shift of the redox potential in dmf.[5,6]

A slight distortion of the $[Fe^{III}(S\text{-}cys)_4]^-$ core in the active site of rubredoxin [7] or its model complexes, $[Fe(PhCH_2OCO\text{-}cys\text{-}Pro\text{-}Leu\text{-}cys\text{-}OMe)_2]^-$,[8] demonstrated on the basis of the observed near-infrared circular dichroism (CD) peaks at 6000 and 7400 cm^{-1} arising from d–d transitions or the appearance of the characteristic magnetic circular dichroism (MCD) band at 28 800 cm^{-1}, due to the ligand-to-metal charge-transfer transition, was taken as evidence of the splitting of the iron(III) d orbitals induced by the chelation effect of Cys-X-Y-Cys (X,Y = amino acid residues).[8] The distortion from D_{2d} to C_2 in the oxidized state has been ascribed to the variation in Fe–S π-bond character with the change in S–Fe–S–C torsion angles which is probably induced by the peptide conformation. This relation between the π interaction and the Fe–S–C torsion angle has been demonstrated using extended-Hückel calculations.[9] These calculation results are consistent with the trend in the crystallographical parameters of the $[Fe(S\text{-}cys)_4]^-$ core in *Clostridium pasteurianum* rubredoxin.[10]

On the other hand, bulky thiolate ligands have been considered to influence inherent properties such as redox stability. For example, $[Fe(SC_6HMe_4\text{-}2,3,5,6)_4]^-$ (ref. 11) and $[Fe_4S_4(SC_6H_2R_3\text{-}2,4,6)_4]^{2-}$ (R = alkyl)[12–14] have been reported to be relatively stable in the oxidized states.

In this paper we describe the synthesis, crystal structure, and spectro- and electro-chemical properties of $[Fe_2S_2(tmbt)_4]^{2-}$ (tmbt = 2,4,6-trimethylbenzenethiolate). The effects of the torsion angle on the Fe–S(C) bond character were examined by extended-Hückel molecular orbital (EHMO) calculations on the simplified model complex $[Fe_2S_2(SH)_4]^{2-}$.

Experimental

Materials and Methods.—All operations were carried out under an argon atmosphere. Solvents were purified by distillation under an argon atmosphere before use. Methanol, acetonitrile, 1,2-dimethoxyethane (dme), diethyl ether, and $[^2H_3]$acetonitrile were purified according to the literature methods.[15] Dimethylformamide (dmf) was distilled under reduced pressure several times before use as a solvent for the electrochemical measurements. Mesitylenesulphonyl chloride was prepared by the reported method.[16] The salt $[NEt_4]_2[Fe_2S_2Cl_4]$ was prepared according to the literature method.[17]

Preparations.—*Bis*(2,4,6-*trimethylphenyl*) *disulphide.* In a three-necked flask (100 cm^3) with a condenser and a dropping funnel was placed a suspension of lithium aluminium hydride (16.1 g, 0.424 mol) in diethyl ether (300 cm^3). A solution of mesitylenesulphonyl chloride (44.2 g, 0.203 mol) in diethyl ether (200 cm^3) was added with vigorous stirring at 5 °C. After the evolution of hydrogen had subsided the reaction mixture was allowed to stand at room temperature for 1 h and then refluxed for 6 h. After treatment with water and 0.5 mol dm^{-3} sulphuric acid, the ether layer was separated and concentrated. The residue was dissolved in ethanol and oxidized by iodine (15 g) to give a pale yellow precipitate. The precipitate was collected by filtration, washed with ethanol and recrystallized from ethanol–acetonitrile. Yield 15.1 g (48%); $\delta_H(CDCl_3)$ 2.18 (s, *o*-CH_3), 2.21 (s, *p*-CH_3) and 6.83 (s, *m*-H) (Found: C, 71.10; H, 7.35; S, 21.00. $C_{18}H_{22}S_2$ requires C, 71.45; H, 7.35; S, 21.25%).

Sodium 2,4,6-*trimethylbenzenethiolate*, Na(tmbt). Sodium metal (0.53 g, 23 mmol) was added to a solution of bis(2,4,6-trimethylphenyl) disulphide (3.5 g, 11.4 mmol) in dme (50 cm^3) at 0 °C. After heating at 40 °C for 1 h the solution was allowed to

† Bis(tetramethylammonium) di-μ-sulphido-bis[bis(2,4,6-trimethylbenzenethiolato)ferrate(III)].

Supplementary data available: see Instructions for Authors, *J. Chem. Soc., Dalton Trans.*, 1991, Issue 1, pp. xviii–xxii.

Table 1 Crystallographic data for $[NEt_4]_2[Fe_2S_2(tmbt)_4]$

Formula	$C_{52}H_{84}Fe_2N_2S_6$
M	1039.29
Colour	Black
Crystal dimensions/mm	0.20 × 0.10 × 0.50
Crystal system	Monoclinic
Crystal shape	Prism
Space group	$P2_1/c$
a/Å	15.241(6)
b/Å	16.174(5)
c/Å	16.768(6)
β/°	135.84(2)
U/Å^3	2879(2)
Z	2
D_c/g cm^{-3}	1.20
μ/cm^{-1}	6.21
$F(000)$	1116
T/°C	21 ± 2
Scan speed/° min^{-1}	4
Octants	$\pm h, k, l$
2θ range/°	0–40
Unique data	2694
Used data [$I_o > 3\sigma(I)$]	1577
Number of parameters	329
R^a	0.073
R'^b	0.082

^{a} $R = \Sigma||F_o| - |F_c||/\Sigma|F_o|$. ^{b} $R' = [\Sigma w(|F_o| - |F_c|)^2/\Sigma w|F_o|^2]^{\frac{1}{2}}$; $w = 1/\sigma^2(|F_o|)$.

Table 2 Atom coordinates and estimated standard deviations for $[NEt_4]_2[Fe_2S_2(tmbt)_4]$

Atom	x	y	z
Fe	0.600 4(2)	0.047 37(14)	0.547 02(17)
S*	0.515 5(4)	−0.051 3(3)	0.419 6(3)
S(1)	0.604 0(5)	0.172 7(3)	0.484 8(4)
S(2)	0.802 1(4)	0.020 5(3)	0.724 7(4)
N(001)	0.721 9(12)	0.422 8(7)	0.451 5(10)
C(11)	0.531 9(14)	0.168 0(9)	0.341 4(12)
C(12)	0.604 0(16)	0.145 8(11)	0.322 0(15)
C(13)	0.550 1(15)	0.156 8(11)	0.209 9(14)
C(14)	0.429 5(16)	0.187 0(9)	0.120 3(13)
C(15)	0.358 6(14)	0.203 8(10)	0.144 2(13)
C(16)	0.405 8(15)	0.193 6(10)	0.251 8(13)
C(121)	0.737 6(16)	0.111 3(13)	0.415 1(15)
C(141)	0.375 5(17)	0.202 5(11)	0.000 8(13)
C(161)	0.321 8(17)	0.211 2(12)	0.268 2(15)
C(21)	0.901 0(12)	0.036 0(10)	0.705 8(11)
C(22)	0.958 4(14)	0.114 8(11)	0.731 0(12)
C(23)	1.036 4(15)	0.125 4(11)	0.716 2(13)
C(24)	1.060 2(14)	0.065 0(12)	0.731 0(12)
C(25)	1.003 3(15)	−0.010 9(12)	0.652 4(13)
C(26)	0.921 7(13)	−0.029 5(10)	0.663 4(12)
C(221)	0.935 9(16)	0.186 6(11)	0.773 0(14)
C(241)	1.145 8(18)	0.077 5(18)	0.657 8(17)
C(261)	0.858 9(16)	−0.113 3(11)	0.632 0(16)
C(011)	0.731 5(15)	0.488 9(9)	0.394 1(12)
C(012)	0.852 5(14)	0.538 1(11)	0.474 3(13)
C(021)	0.717 2(18)	0.466 6(12)	0.531 7(15)
C(022)	0.693(3)	0.408 4(14)	0.587 0(18)
C(031)	0.598 1(16)	0.374 9(11)	0.357 9(14)
C(032)	0.477 9(16)	0.424 1(12)	0.288 5(15)
C(041)	0.832 1(19)	0.360 7(13)	0.518 2(17)
C(042)	0.859(3)	0.324 2(14)	0.456 9(19)

stand at room temperature overnight. The product precipitated as white needles (4.3 g), and was collected by filtration, washed with hexane, and dried over sodium hydroxide *in vacuo*; $\delta_H(C_6D_6)$ 2.81 (s, *o*-CH_3), 2.93 (s, *p*-CH_3) and 7.00 (s, *m*-H).

$[NEt_4]_2[Fe_2S_2(tmbt)_4]$. An acetonitrile solution (50 cm^3) of Na(tmbt) (1.1 g, 3.3 mmol) was added to a solution of $[NEt_4]_2[Fe_2S_2Cl_4]$ (0.46 g, 0.8 mmol) in acetonitrile (100 cm^3). The mixture was stirred for 1 h, filtered, and the filtrate concentrated *in vacuo*. The residue was washed with a small amount of cold methanol and dried *in vacuo*. The crude product was recrystallized by dissolution in acetonitrile (50 cm^3) and slow cooling to 0 °C. Air-sensitive black prisms were obtained (67%) (Found: C, 59.45; H, 8.05; N, 2.75. $C_{52}H_{84}Fe_2N_2S_6$ requires C, 60.00; H, 8.15; N, 2.70%).

X-Ray Diffraction Measurements and Data Collection.—The crystal of $[NEt_4]_2[Fe_2S_2(tmbt)_4]$ sealed in a glass capillary under argon was mounted on a Rigaku AFC-C-4 automated four-circle diffractometer for data collection and processing at room temperature using graphite-monochromatized Mo-Kα radiation. Lorentz and polarization corrections were applied but no correction was made for absorption. The unit-cell dimensions were obtained from 20 reflections ($10 < 2\theta < 20°$) and refined with 25 other reflections ($2\theta > 20°$). Three standard reflections were monitored with every 100 and did not show any significant change. The positions of the Fe and S atoms were determined by the direct method (MULTAN 80).[18] Subsequent Fourier syntheses based on the phases of the Fe and S atoms revealed the positions of the remaining non-hydrogen atoms. The refinement with anisotropic thermal parameters converged at $R = 0.0729$, which is still high because of the positional disorder of the tetraethylammonium cation. Atom scattering factors were taken from ref. 19.

Crystal data are listed in Table 1, atomic coordinates of the non-hydrogen atoms and their estimated standard deviations in Table 2. Atoms, N(001) and C(011)–C(042) belong to the counter cation, NEt_4^+.

Additional material available from the Cambridge Crystallographic Data Centre comprises H-atom coordinates, thermal parameters and remaining bond lengths and angles.

Physical Measurements.—Absorption spectra were recorded on a JASCO UVIDEC-5A spectrophotometer with a 1 mm cell. The sample solution was 8×10^{-4} mol dm^{-3}. The ^{1}H NMR spectra were obtained on JEOL FX-90Q and FX-200 spectrometers at 23 °C, respectively. Cyclic voltammetry was performed on a YANACO P8-CV instrument equipped with a YANACO model FG-1218 function generator. The voltammograms were obtained at room temperature with a three-electrode system consisting of a glassy-carbon working electrode, a platinum-wire auxiliary electrode, and a saturated calomel electrode (SCE) as the reference. The salt $[NBu^n_4][ClO_4]$ was employed as a supporting electrolyte. The measurements were carried out at several scanning rates (50–200 mV s^{-1}). The value of $E_{\frac{1}{2}}$ was estimated from $(E_{p_c} + E_{p_a})/2$.

Extended-Hückel Molecular-orbital Calculations.—In these calculations D_{2h} symmetry was assumed for the Fe_2S_4 portion of the compound with tetrahedral geometry for the two iron(III) ions as found in the structure of $[Fe_2S_2(SC_6H_4Me\text{-}p)_4]^{2-}$.[2] The following geometrical parameters were used: Fe–S* (inorganic sulphide) 2.201, Fe–S(H) 2.305, S–H 1.34 Å; Fe–S*–Fe 75.39, S*–Se–S 110.27, Fe–S–H 109.5°. The extended-Hückel parameters for Fe were taken from earlier work,[20] and those for S and H are the standard ones. Table 3 summarizes the parameters used.

Results and Discussion

Structure of $[NEt_4]_2[Fe_2S_2(tmbt)_4]$.—This complex crystallizes in space group $P2_1/c$ in the monoclinic system with two formula units per unit cell (Table 1). The structure of the anion is shown in Fig. 1. Selected interatomic distances and angles are collected in Table 4. The complex contains a normal $Fe_2S_2^{2+}$ core having a planar structure as in $[Fe_2S_2(SC_6H_4Me\text{-}p)_4]^{2-}$.[2] The two Fe–S* distances are 2.195(6) and 2.204(6) Å. The Fe ··· Fe distance [2.698(5) Å] resembles that [2.698(1) Å] of $[Fe_2S_2\{o\text{-}(SCH_2)_2C_6H_4\}_2]^{2-}$.[2] The two terminal Fe–S(C)

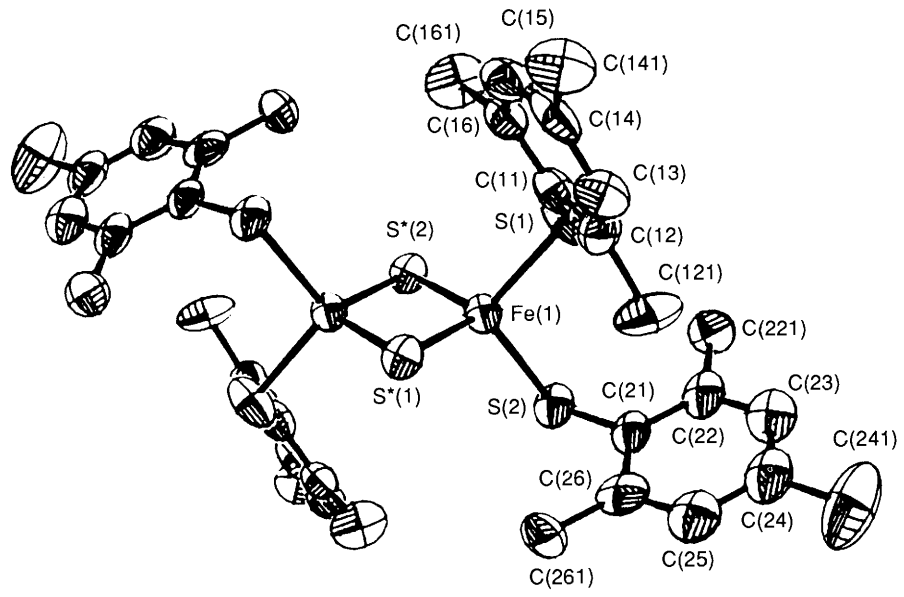

Fig. 1 Crystal structure of $[Fe_2S_2(tmbt)_4]^{2-}$ showing 50% probability ellipsoids

Table 3 Hückel parameters (eV ≈ 1.60 × 10^{-19} J)

Orbital		H_{ii}/eV	ζ_1
Fe	4s	−8.39	1.9
	4p	−4.74	1.9
	3d*	−11.46	5.35
S	3s	−20.00	1.817
	3p	−13.30	1.817
H	1s	−13.6	1.3

* Exponents and coefficients used in double-zeta expansion: ζ_2 = 1.8, C = 0.5366 and C_2 = 0.6678.

Table 4 Selected interatomic distances (Å) and angles (°) of $[Fe_2S_2(tmbt)_4]^{2-}$

Fe(1)–S*(1)	2.195(6)	S*(1)···S*(2)	3.475(8)
Fe(1)–S*(2)	2.204(6)	S(1)···S(2)	3.733(9)
Fe(1)–S(1)	2.299(8)	S(1)–C	1.790(22)
Fe(1)–S(2)	2.318(6)	S(2)–C	1.767(19)
Fe(1)···Fe(2)	2.698(5)		
S*(1)–Fe(1)–S*(2)	104.35(23)	S(1)–Fe(1)–S(2)	107.89(25)
S*(1)–Fe(1)–S(1)	112.84(26)	Fe(1)–S*(1)–Fe(2)	75.65(20)
S*(1)–Fe(1)–S(2)	115.28(23)	Fe(1)–S(1)–C	112.35(76)
S*(2)–Fe(1)–S(2)	104.13(23)	Fe(1)–S(2)–C	104.95(64)
S*(2)–Fe(1)–S(1)	112.02(26)		
S*(1)–Fe–S(1)–C		S*(1)–Fe–S(2)–C	
1.98 (ψ = 58.0)		50.60 (ψ = −9.4)	

bonds are 2.318(6) and 2.299(8) Å, close to the value [2.312(1) Å] in $[Fe_2S_2(SC_6H_4Me\text{-}p)_4]^{2-}$.

The Fe–S–C angles in $[Fe_2S_2(tmbt)_4]^{2-}$ were found to be 112.35(76) and 104.95(64)°. The S*–Fe–S(C) angles [112.84(26), 115.28(23) and 104.13(23)°, 104.35(23)°] reflect the same trend. The systematic study of thiophenolate and selenophenolate metal complexes has revealed that the M–X–C (M = Zn^{II} or Cd^{II}, X = S or Se) angles reflect the M–X bond character.[21] Large M–S–C angles (*ca.* 109°) have been reported for $[M(SPh)_4]^{2-}$ (M = Co^{II}, Ni^{II} or Mn^{II}).[22] A large Fe–S–C angle (mean 110.9°) was also reported for $[Fe(SPh)_4]^{2-}$ and can be interpreted as due to the highly covalent nature of the bond between Fe^{II} and S(C).[23]

The two different orientations of the aromatic thiolate ligands arise from the steric congestion with methyl groups at the *ortho* positions of the aromatic ring. The sulphur p_π orbitals are incapable of overlapping with the π system of two of the four aromatic rings because the Fe–S–C planes are perpendicular to their phenyl plane, although all Fe–S–C groups and aromatic rings in $[Fe_2S_2(SC_6H_4Me\text{-}p)_4]^{2-}$ are coplanar.[3] The two aromatic rings in $[Fe_2S_2(tmbt)_4]^{2-}$ bend toward $Fe_2S_2^{2+}$.

Two sets of S*–Fe–S–C torsion angles (1.98 and 50.60°) were observed as listed in Table 4. Generally, a S*–Fe–S–C dihedral angle of 60° (ψ = 0°) is conformationally preferable corresponding to the staggered position in ideal D_{2h} symmetry, as shown by the crystal structures of $[Fe_2S_2(SPh)_4]^{2-}$ (ref. 2) and $[Fe_2S_2(SC_6H_4Me\text{-}p)_4]^{2-}$.[3] The extraordinarily small torsion angle (1.98°, ψ = 58.02°) at the eclipsed position corresponds to the large Fe–S–C angle [112.35(76)°]. In the case of $[Fe_4S_4(tmbt)_4]^{2-}$ all of the four S*–Fe–S–C torsion angles (mean 26.45°) with four small Fe–S–C angles [two sets of 99.4(7) and 100.4(5)°] are rotated into the eclipsed position.[13] In this case the Fe–S–C angle with the eclipsed S*–Fe–S–C torsion angle becomes smaller than that of the corresponding thiophenolate complex. However, the trend for $[Fe_2S_2(tmbt)_4]^{2-}$ is opposite to that in the relation between the Fe–S–C angle and the S*–Fe–S–C torsion angle, and is similar to that for the $Fe(S\text{-}cys)_4$ core of native rubredoxin according to X-ray analysis.[10] The change of S*–Fe–S–C torsion angle varies the Fe–S bond character with respect to the degree of π interaction between the Fe d and S p orbitals as discussed below.

Electronic Spectra.—The salt $[NEt_4]_2[Fe_2S_2(tmbt)_4]$ in dmf exhibits well resolved absorption maxima (Fig. 2) at 434 (17 600) and 346 nm (16 900 dm^3 mol^{-1} cm^{-1}) which are unusually blue-shifted compared with those of other *p*-substituted benzenethiolato 2Fe–2S complexes.[2] The addition of 8 equivalents of benzenethiol to a dmf solution of the complex resulted in the appearance of a broad maximum at 490 nm (11 000 dm^3 mol^{-1} cm^{-1}) with a shoulder (540 nm) which corresponds to the reported spectral data for $[Fe_2S_2(SPh)_4]^{2-}$.[2] The blue-shifted absorption maximum (434 nm) is distinct from the ligand-to-metal charge-transfer (l.m.c.t.) absorption maxima (482–502 nm) for complexes having *p*-substituted benzenethiolate ligands. Holm and co-workers[2] pointed out that the l.m.c.t. band of $[Fe_2S_2(SC_6H_4X\text{-}p)_4]^{2-}$ (X = Cl, H or Me) red-shifts in the order of X = Cl < H < Me due to the increasing inductive effect of the X group.[2] The blue shift of the l.m.c.t. absorption maximum for $[Fe_2S_2(tmbt)_4]^{2-}$ is ascribed to the steric prevention of π interaction between sulphur and the aromatic ring. This trend

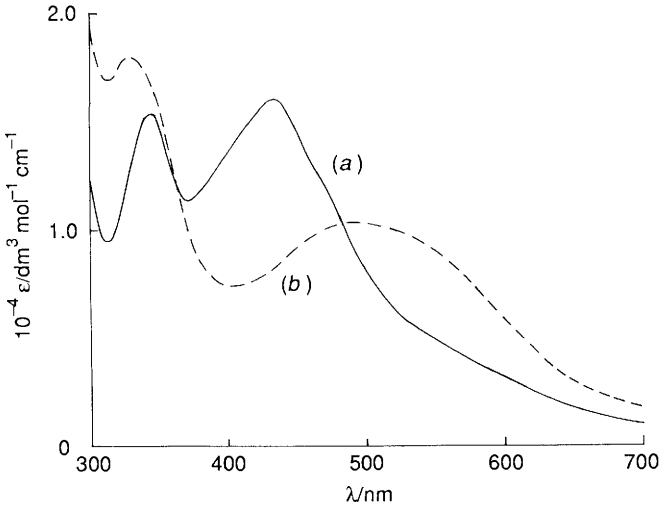

Fig. 2 Absorption spectra of (*a*) $[NEt_4]_2[Fe_2S_2(tmbt)_4]$ (5×10^{-4} mol dm^{-3}) in dmf and (*b*) after core extrusion by thiophenol (5×10^{-3} mol dm^{-3}) from solution (*a*)

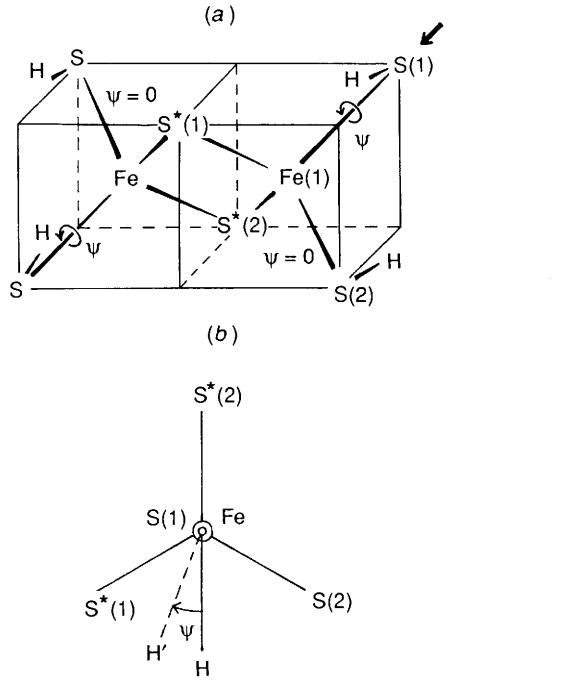

Fig. 3 (*a*) Illustration of $[Fe_2S_2(SH)_4]^{2-}$ in D_{2h} symmetry. (*b*) Definition of Fe–S(H) torsion angles (ψ)

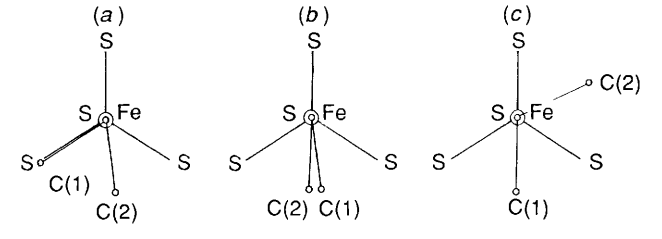

Fig. 4 Illustration of the various S*–Fe–S–C torsion angles for (*a*) $[Fe_2S_2(tmbt)_4]^{2-}$, (*b*) $[Fe_2S_2(SC_6H_4Me\text{-}p)_4]^{2-}$ and (*c*) $[Fe_2S_2\{o\text{-}(SCH_2)_2C_6H_4\}_2]^{2-}$

has been also observed in the case of an analogous 4Fe–4S complex, $[Fe_4S_4(tmbt)_4]^{2-}$ in dmf,[12] although the absorption maximum at 425 nm (19 100 dm^3 mol^{-1} cm^{-1}) reported for $[FeS_2(btpo)_2]^{2-}$ [btpo = 2,2′-bis(thiophenolate)] is blue shifted without the π interaction between sulphur and the aromatic ring.[24]

^{1}H *NMR Spectra*.—The chemical shifts of *o*- or *p*-substituted benzenethiolato $Fe_2S_2^{2+}$ complexes were compared using the isotropic shifts $(\Delta H/H_0)_{iso}$ reported by Reynolds and Holm.[17] The isotropic shifts of $[Fe_2S_2(tmbt)_4]^{2-}$ in [$^2H_3$]acetonitrile at 23 °C were found to be −3.47, −3.06 and −4.24 for *o*-CH_3, *m*-H and *p*-CH_3, respectively. The complexes $[Fe_4S_4(SPh)_4]^{2-}$ and $[Fe_4S_4(SC_6H_4Me\text{-}o)_4]^{2-}$ have been reported to exhibit isotropic shifts of −2.11 and −2.10 for *m*-H, respectively, and of −3.74 for *p*-CH_3.[16] The large isotropic shifts are expected due to the weaker antiferromagnetic interaction between the two iron(III) ions of $Fe_2S_2^{2+}$, when compared to those of $[Fe_4S_4(tmbt)_4]^{2-}$ (−1.15 to −1.45).[13] The isotropic shifts of *m*-H and *p*-CH_3 in $[Fe_4S_4(tmbt)_4]^{2-}$ were found to be larger than those of $[Fe_4S_4(SC_6H_4Me\text{-}o)_4]^{2-}$. The larger contact shift through Fe–S–C–C–C–C is quite noticeable because of steric prevention of the π interaction between sulphur and the phenyl ring. Probably either of the two kinds of Fe–S(C) bonds contributes to the larger contact shift, although a fast exchange between the two bonds occurs in solution.

Electrochemical Properties.—The ion $[Fe_2S_2(tmbt)_4]^{2-}$ exhibits a 3−/2− redox couple at −0.87 V *vs.* SCE in dmf or at −1.15 V *vs.* SCE in dme which are irreversible ($i_{p,a}/i_{p,c} = 0.75$ or 0.50, respectively). The irreversible redox couple is accompanied by a new reversible redox couple at −1.40 V *vs.* SCE. The instability of the electrochemically reduced species, $[Fe_2S_2(tmbt)_4]^{3-}$, leads to formation of $[Fe_4S_4(tmbt)_4]^{2-}$ by decomposition. This reaction is known for the chemical reduction of some 2Fe–2S complexes.[25]

The redox potentials of $[Fe_2S_2(SPh)_4]^{2-}$, $[Fe_2S_2(SC_6H_4Me\text{-}p)_4]^{2-}$ and $[Fe_2S_2(SC_6H_4NMe_2\text{-}p)_4]^{2-}$ have been reported to be at −1.09, −0.97 and −0.83 V *vs.* SCE, respectively in dmf.[2] Mayerle *et al.*[2] found a correlation between the redox potential and the Hammett σ constants of the substituent of benzenethiolate ligands. The electron-withdrawing effect of the phenyl group contributes to the positive shift of the redox potential. In the case of the tmbt complex the electron-donating methyl substituents are expected to shift the redox potential to more negative values. However, $[Fe_2S_2(tmbt)_4]^{2-}$ shows a clear positive shift in dmf. The crystal structure of $[Fe_2S_2(tmbt)_4]^{2-}$ indicates that the Fe–S–C plane is perpendicular to the phenyl plane and that the sulphur p_π orbital does not conjugate with the phenyl π system. Thus, the electron-donating effect of the methyl groups at the *ortho* and *para* positions is almost completely offset.

Evaluation of the Torsion-angle Dependence of the Fe–S *Bond Character by MO Calculation*.—Extended-Hückel MO calculations were performed on $[Fe_2S_2(SH)_4]^{2-}$ with variation of two of the four S*–Fe–S–H torsion angles in the same direction as the crystal structure of $[Fe_2S_2(tmbt)_4]^{2-}$ with two eclipsed S*–Fe–S–C torsion angles in C_2 symmetry. The two sets of five electrons at each iron centre gave the lowest orbitals in turn when a diamagnetic $Fe_2S_2^{2+}$ centre was assumed for the calculations. Fig. 3 shows a schematic drawing of the structure of the model complex ion $[Fe_2S_2(SH)_4]^{2-}$. This geometry is taken from the symmetrical structure (D_{2h}) of $[Fe_2S_2(SC_6H_4Me\text{-}p)_4]^{2-}$ which has a staggered Fe–S(C) torsion angle ($\psi \approx 0°$), that is a S*–Fe–S–C dihedral angle of 60° illustrated in Fig. 4. The staggered Fe–S(C) position ($\psi = 0$) is defined as that of the C atom in the (S*)Fe–S(C) bond with the smallest steric hindrance. Two of the S*–Fe–S–H torsion angles of $[Fe_2S_2(SH)_4]^{2-}$ were rotated to the same direction shown in Fig. 5. The S*–Fe–S–H torsion angle dependence of the overlap population for the two sets of Fe–S(H) bonds [Fe(1)–S(1), Fe(1)–S*(1), Fe(1)–S(2) and Fe(1)–S*(2)] is also shown in Fig. 5. The overlap population of the Fe(1)–S(1) bond with various torsion angles was calculated to exhibit a maximum at $\psi = 60°$ (eclipsed form), when the overlap population of the Fe(1)–S(2) bond with $\psi = 0°$ (staggered form) is lowered. The results are consistent with the crystal structure parameters for

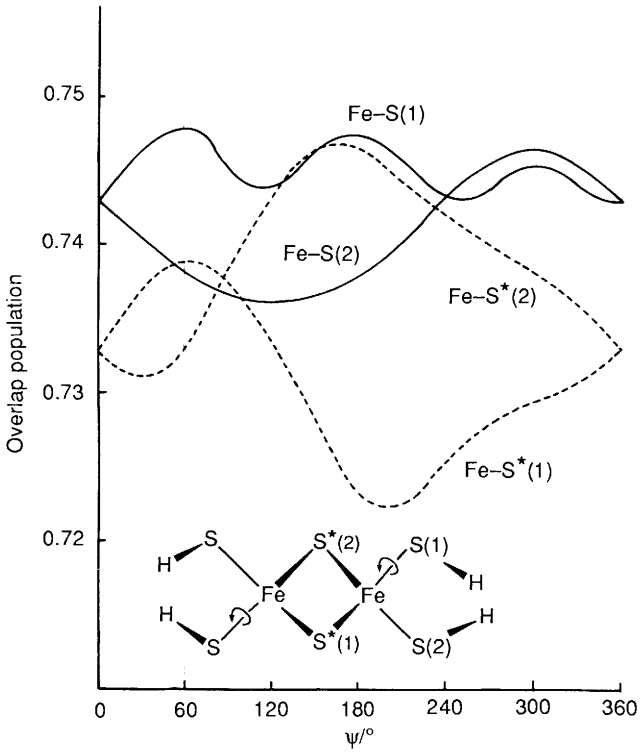

Fig. 5 Variation of the Fe–S(H) overlap populations with change in two of the four Fe–S(H) torsion angles. The dashed line indicates the Fe(1)–S(1) torsion angle ($\psi = 60°$) in $[Fe_2S_2(tmbt)_4]^{2-}$

$[Fe_2S_2(tmbt)_4]^{2-}$ although the large standard deviation of the Fe–S(C) bond distances does not allow us to discuss the bond character directly.

The larger Fe–S–C angle [112.35(76)°] corresponds to the eclipsed torsion angle ($\psi = 58.02°$), the smaller Fe–S–C angle [104.95(64)°] to a staggered Fe–S torsion angle ($\psi = -9.4°$). The former is ascribed to the large π character of the Fe–S(C) bond as discussed for $[Zn(SPh)_4]^{2-}$ (ref. 21) and for the crystallographic results of *Clostridium pasteurianum* rubredoxin.[26]

The variation in the energy of the iron(III) d orbitals with rotation of the Fe–S(H) bond was estimated for $[Fe_2S_2(SH)_4]^{2-}$. When the complex is assumed to have a diamagnetic electron configuration the energy level of the lowest unoccupied orbital (LUMO) decreases with increasing Fe–S(H) torsion angle. Thus, the decrease in the LUMO energy is associated with the positive shift (−0.87 V *vs.* SCE) of the reduction potential, compared with those of the corresponding arenethiolate complexes, *e.g.* −0.97 V *vs.* SCE for $[Fe_2S_2(SC_6H_4Me\text{-}o)_4]^{2-}$.

The importance of such variations with the SR orientation (variation of S*–Fe–S–C torsion angle) as regards the electronic structure including the charge and spin-density distributions has been suggested from LCAO-Xα valence bond[27] and spin-unrestricted MO calculations on $[Fe_2S_2(SH)_4]^{2-}$.[28]

The crystallographic structure of $[Fe_2S_2(S\text{-}cys)_4]^{2-}$ in *Spirulina platensis* ferredoxin is similar to the parent D_{2h} geometry used for the calculations. Only one Fe–S(C) torsion angle [Cys(49)] is rotated from the staggered position to an eclipsed one and the others [Cys(42) and Cys(47)] are normal.[29] The Fe–S overlap populations will change with variation of one [Fe(1)–S(2)] of the four Fe–S torsion angles in $[Fe_2S_2(S\text{-}cys)_4]^{2-}$. On the other hand, the thiolate sulphurs of Cys(47) and Cys(42) were reported to form NH • • • S hydrogen bonds with the amide groups of the Cys-A-B-C-D-Cys-X-Y-Cys sequence (A–D, X, Y are amino acid residues).[30] The formation of the NH • • • S hydrogen bonds also results in decreasing Fe–S overlap population because of the apparent decrease in lone-pair electron density at sulphur. Thus, to discuss the precise effect of the restrictedly rotated Fe–S(C) bond at the Cys(49) of plant-type ferredoxin, further study is required.

Conclusion

The complex $[NEt_4]_2[Fe_2S_2(tmbt)_4]$ has two large and two small Fe–S–C angles. The deviation of the Fe–S(C) torsion angles from the stable staggered ones in $[Fe_2S_2(SR)_4]^{2-}$ varies all of the Fe–S(C) bond characters. The effect of the restrictedly rotated Fe–S(C) on the Fe–S bond properties was established by extended-Hückel MO calculations with a $[Fe_2S_2(SH)_4]^{2-}$ model. A study of the conformational preference of Fe–S(Cys) bonding from a characteristic peptide sequence is thus important and will be continued further to clarify the biological regulation by the macrocyclic peptide chelation.

References

1 W. H. Orme-Johnson, *Annu. Rev. Biochem.*, 1973, **42**, 159.
2 J. J. Mayerle, S. E. Denmark, B. V. Depamphilis, J. A. Ibers and R. H. Holm, *J. Am. Chem. Soc.*, 1975, **97**, 1032.
3 M. A. Bobrik, K. O. Hodgson and R. H. Holm, *J. Am. Chem. Soc.*, 1977, **16**, 1851.
4 P. Beardwood and J. F. Gibson, *J. Chem. Soc., Dalton Trans.*, 1984, 1507.
5 N. Ueyama, S. Ueno, M. Nakata and A. Nakamura, *Bull. Chem. Soc. Jpn.*, 1984, **57**, 984.
6 S. Ueno, N. Ueyama, A. Nakamura and T. Tsukihara, *Inorg. Chem.*, 1986, **25**, 1000.
7 W. A. Eaton and W. Lovenberg, *Iron-Sulfur Proteins*, ed. W. Lovenberg, Academic Press, New York, 1973, vol. 2, p. 131.
8 M. Nakata, N. Ueyama and A. Nakamura, *Bull. Chem. Soc. Jpn.*, 1983, **56**, 3647.
9 N. Ueyama, T. Sugawara, K. Tatsumi and A. Nakamura, *Inorg. Chem.*, 1987, **26**, 1978.
10 K. D. Watenpaugh, L. C. Sieker and L. H. Jensen, *J. Mol. Biol.*, 1979, **131**, 509.
11 M. M. Millar, J. F. Lee, S. A. Koch and R. Fikar, *Inorg. Chem.*, 1982, **21**, 4106.
12 N. Ueyama, T. Terakawa, T. Sugawara, M. Fuji and A. Nakamura, *Chem. Lett.*, 1984, 1287.
13 N. Ueyama, T. Sugawara, M. Fuji, A. Nakamura and N. Yasuoka, *Chem. Lett.*, 1985, 175.
14 T. O'Sullivan and M. M. Millar, *J. Am. Chem. Soc.*, 1985, **107**, 4096.
15 C. K. Mann, *Electroanal. Chem.*, 1963, 3.
16 G. B. Wong, M. A. Bobrik and R. H. Holm, *Inorg. Chem.*, 1978, **17**, 578.
17 J. G. Reynolds and R. H. Holm, *Inorg. Chem.*, 1980, **19**, 3257.
18 P. Main, M. M. Woolfson and G. Germain, MULTAN 80, A Computer Program for the Automatic Solution of Crystal Structures, Universities of York and Louvain, 1971.
19 D. T. Cromer and J. T. Waber, *International Tables for X-Ray Crystallography*, Kynoch Press, Birmingham, 1974, vol. 4, Table 2.2 A.
20 K. Tatsumi and R. Hoffmann, *J. Am. Chem. Soc.*, 1981, **103**, 3328.
21 N. Ueyama, T. Sugawara, K. Sasaki, A. Nakamura, S. Yamazaki, Y. Wakatsuki, H. Yamazaki and N. Yasuoka, *Inorg. Chem.*, 1988, **27**, 741.
22 D. Swenson, N. C. Baenzinger and D. Coucouvanis, *J. Am. Chem. Soc.*, 1978, **100**, 1933.
23 D. Coucouvanis, D. Swenson, N. C. Baenzinger, C. Murphy, D. G. Sfarnas, A. Simopoulos and A. Kostikas, *J. Am. Chem. Soc.*, 1981, **103**, 3350.
24 P. Beardwood and J. F. Gibson, *J. Chem. Soc., Dalton Trans.*, 1983, 737.
25 J. Cambray, R. W. Lane, A. G. Wedd, R. W. Johnson and R. H. Holm, *Inorg. Chem.*, 1977, **16**, 2565.
26 K. D. Watenpaugh, L. C. Sieker and L. H. Jensen, *J. Mol. Biol.*, 1979, **131**, 509.
27 L. Noodleman and E. J. Bearends, *J. Am. Chem. Soc.*, 1984, **106**, 2316.
28 R. Bläs, E. Bill, S. Lauer, A. X. Trautwein, H. Winkler, M. Grodzicki and A. Kostikas, *Frontiers in Bioinorganic Chemistry*, ed. A. V. Xavier, VCH, Weinheim, 1986, p. 515.
29 T. Tsukihara, personal communication.
30 T. Tsukihara, K. Fukuyama, H. Tahara, Y. Katsube, Y. Matsubara, N. Tanaka, M. Kakudo, K. Wada and H. Matsubara, *J. Biochem.*, 1978, **84**, 1645.

Received 27*th February* 1991; *Paper* 1/00931A